



QUANTITATIVE SEISMIC RISK ASSESSMENT OF WOOD-FRAME BUILDINGS IN RICHMOND, BRITISH COLUMBIA

Katsuichiro Goda¹ and Gail M. Atkinson²

ABSTRACT

An accurate assessment of aggregate seismic loss of structures and infrastructure is the key to successful earthquake risk management. For this, a seismic risk model for multiple buildings is developed by incorporating new ground motion models, spatial correlation models of seismic excitations, and peak inelastic ductility models of degrading structural systems with pinching behavior, and is then applied to 1574 existing wood-frame buildings in Richmond, British Columbia. The analysis results identify the use of an adequate spatial correlation model of peak ground motions and the determination of the expected seismic capacity as the most significant model components. Therefore, they should be examined and elaborated more thoroughly in future investigations.

Introduction

Buildings and infrastructure are the fundamental backbone of urban cities and economic activities. From the point of view of earthquake risk management, decision makers who are concerned with the seismic performance of multiple structures in their jurisdiction must take simultaneous seismic effects on the assets and facilities into account, as they are correlated in both time and space. The spatiotemporally-correlated seismic excitations accelerate the concentration of seismic losses in a small region, resulting in potentially-catastrophic consequences.

Recently, a simulation-based seismic risk model for multiple buildings was developed by Goda and Hong (2008b), which consists of four main components: 1) earthquake occurrence and ground motion prediction, 2) inelastic seismic demand estimation, 3) seismic vulnerability assessment, and 4) seismic loss estimation and decision-making. This framework has advantages over other existing models/methods, such as HAZUS-MH (FEMA and NIBS 2003), in that uncertain occurrences of all possible earthquakes as well as spatiotemporally-correlated seismic effects are explicitly taken into account. Thus, the aggregate seismic loss of multiple buildings can be assessed more accurately.

¹Lecturer, Dept. of Civil Engineering, University of Bristol, Bristol, United Kingdom BS8 1TR

²Professor, Dept. of Earth Sciences, University of Western Ontario, London, ON, Canada N6A 5B7

This study extends the original Goda-Hong seismic risk model for multiple buildings by incorporating: i) an updated seismic hazard model for western Canada (Goda et al. 2010), ii) a spatial correlation model of peak ground motions in a subduction environment (Goda and Atkinson 2009a), and iii) prediction models of inelastic seismic demands that account for hysteretic characteristics of degrading structural systems (Goda et al. 2009; Goda and Atkinson 2009b). We apply the updated seismic risk model to 1574 existing wood-frame buildings located in Richmond, British Columbia, and carry out quantitative seismic loss estimation. To assess the impact of the updated model components, comparative investigations are carried out. More specifically, sensitivities of the estimated aggregate seismic loss to: i) different ground motion prediction equations in seismic hazard analysis, ii) different spatial correlation models of peak ground motions and response spectra, and iii) hysteretic characteristics as well as ultimate seismic capacity of a wood-frame structure with degradation and pinching behavior, are investigated quantitatively. Such investigations identify the most influential model components of the developed seismic risk model, and are thus useful for directing efforts in future studies to improve the model.

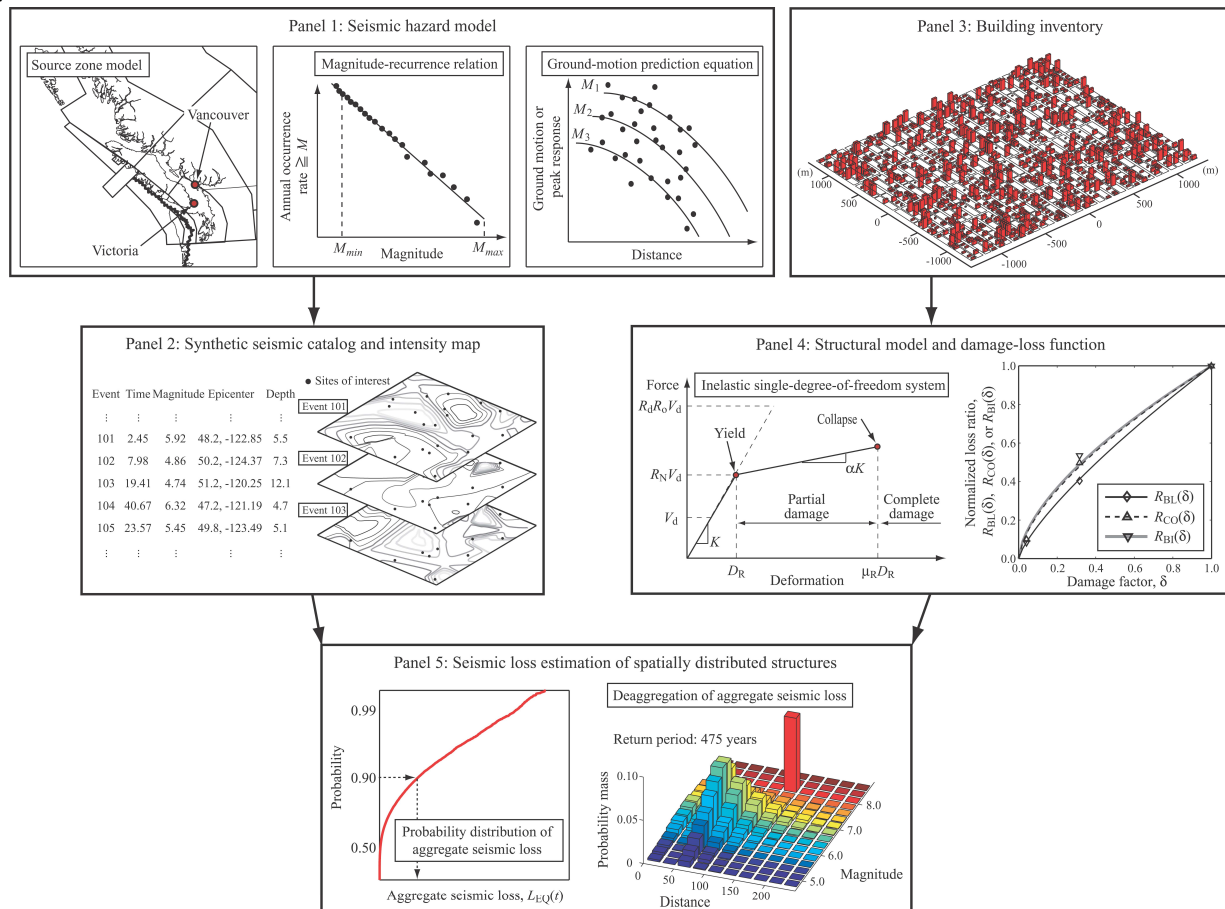


Figure 1. Seismic loss estimation procedure: Panel 1) seismic hazard model, Panel 2) synthetic seismic catalog and intensity map, Panel 3) building inventory, Panel 4) seismic vulnerability assessment, and Panel 5) seismic loss estimation.

Seismic Risk Model for Wood-frame Buildings

Framework

The seismic risk model for multiple buildings consists of five components which are illustrated in Fig. 1: 1) seismic hazard model, 2) synthetic seismic catalog and intensity map, 3) building inventory, 4) seismic vulnerability assessment, and 5) seismic loss estimation of multiple buildings. In the following, we summarize salient features of the seismic risk model; more detailed information is available in Goda and Hong (2008b). Then, we present updated model components of the framework in the subsequent section.

Probabilistic seismic hazard analysis characterizes elastic seismic demand in terms of the spectral acceleration, and incorporates earthquake occurrence models, seismic source zones, magnitude-recurrence relations, and ground motion prediction equations (GMPEs) (Panel 1 in Fig. 1). For western Canada, the seismic hazard information given by Adams and Halchuk (2003) is especially relevant, as it forms the basis of the current national seismic hazard maps of Canada. The seismic hazard model is used to produce a synthetic earthquake catalog and seismic intensity maps for events contained in the synthetic catalog (Panel 2 in Fig. 1). The seismic intensity map for each seismic event is generated by taking spatially-correlated spectral accelerations at multiple sites into account.

Building inventory information includes location, structural and material type, age, story number, occupancy type, floor area, value, and local soil condition, and is the key input for accurate seismic risk assessment (Panel 3 in Fig. 1). Based on the information, an idealized structural model and an adequate structural analysis method are selected for seismic vulnerability assessment. For computational efficiency, each building is represented by an inelastic single-degree-of-freedom (SDOF) system; a statistical model, which is developed based on numerous nonlinear dynamic simulations of an inelastic SDOF system subject to seismic excitations, is adopted to estimate the peak inelastic ductility demand μ_D . The structural capacity is characterized by a force-deformation curve (Panel 4 in Fig. 1), for which yield displacement capacity D_R and ultimate ductility capacity μ_R are defined. By comparing the seismic demand μ_D with the seismic capacity μ_R , a damage factor δ , which is defined as the ratio of $\mu_D - 1$ to $\mu_R - 1$ and ranges between 0 and 1, is evaluated for each building due to an earthquake, and is used to calculate seismic damage costs for different loss categories (Panel 4 in Fig. 1).

We repeat the seismic loss estimation procedure described above for all buildings and for all seismic events included in the synthetic catalog to obtain samples of the aggregate seismic loss $L_{EQ}(t)$ during a period of t years. The seismic loss samples can be used to construct the probability distribution of $L_{EQ}(t)$ (i.e., seismic risk curve) and to identify significant scenario events through deaggregation analysis (Panel 5 in Fig. 1).

Updated Model Components

We succinctly describe features of updated components of the aforementioned seismic risk model for multiple buildings: i) an updated seismic hazard model for western Canada (Goda et al. 2010); ii) a spatial correlation model of peak ground motions in a subduction environment

(Goda and Atkinson 2009a); iii) the use of realistic building inventory information of wood-frame buildings in Richmond, British Columbia; and iv) prediction models of the peak inelastic seismic demand, which account for various hysteretic characteristics of structural systems with degradation and pinching behavior (Goda et al. 2009; Goda and Atkinson 2009b).

Updated Seismic Hazard Model for Western Canada

The availability of new seismic information and seismological models warrants the updating of the seismic hazard model for Canada, as the current Geological Survey of Canada (GSC) model (Adams and Halchuk 2003) was developed in the early 1990s. In particular, improvements can be readily made by using a uniform moment magnitude scale for the earthquake catalog, re-computing the magnitude-recurrence relations for different earthquake types, updating the GMPEs, and using an extended source model rather than a point source model (Goda et al. 2010). The sensitivity analysis results indicate that the use of a suite of recently-developed GMPEs (accounting for epistemic uncertainty) has significant impact on seismic hazard estimates, whereas the implementation of proper distance measure conversion in evaluating GMPEs (Scherbaum et al. 2004) has moderate impact on seismic hazard estimates. (Note: Adams and Halchuk (2003) adopted a single GMPE for each earthquake type and applied epistemic multiplication factors in a logic tree approach; they did not implement finite-fault distance conversion when implementing the GMPEs). In this study, we use the updated seismic hazard model for western Canada. A list of the adopted GMPEs for different earthquake types, which have the most significant impact on seismic hazard assessment among the model components, is given in Table 1; see Goda et al. (2010) for details of other model components.

Table 1. List of the adopted GMPEs for the updated seismic hazard model.

Earthquake type	Ground motion prediction equation	Weight
Shallow crustal earthquakes	[Atkinson (2005), Hong and Goda (2007), Boore and Atkinson (2008)]	[0.25, 0.25, 0.5]
Inslab subduction earthquakes	[Atkinson and Boore (2003)*, Zhao et al. (2006), Goda and Atkinson (2009a)]	[0.5, 0.25, 0.25]
Interface subduction earthquakes	[Gregor et al. (2002), Atkinson and Boore (2003)**, Zhao et al. (2006), Atkinson and Macias (2009)]	[0.25, 0.25, 0.25, 0.25]

* Both global and Cascadia coefficients are used with an equal weight.

** The Cascadia coefficient only is used.

Spatial Correlation Model for Earthquakes in a Subduction Environment

The consideration of an adequate spatial correlation model of spectral accelerations at different sites can have significant impact on the probability distribution of aggregate seismic loss of multiple buildings (Goda and Hong 2008b), and is thus important for accurate seismic loss estimation. A new spatial correlation model has been developed by Goda and Atkinson (2009a) for Japanese earthquakes, which may be applicable to inslab and interface subduction earthquakes in western Canada. Compared with the spatial correlation model for California

earthquakes (Goda and Hong 2008a), the Goda-Atkinson model predicts a higher degree of correlation for the same separation distance between two sites. Hence, the use of the Goda-Atkinson model implies more concentrated seismic losses from multiple buildings.

Inventory of 1574 Wood-frame Buildings in Richmond, British Columbia

Accurate and detailed building inventory information is essential for realistic seismic loss estimation. We collected information for buildings located within three city blocks (each block is about 1 km by 1 km) in the City of Richmond, British Columbia (Fig. 2). The information includes location, year built, story number, structural type, use type, floor area, value, and other relevant data. As the majority of buildings that are contained in the inventory are wood-frame structures, we focus on 1574 wood-frame buildings (out of 1599 buildings included in the database). The occupancy types of the buildings are mostly residential (i.e., single-family dwelling and multi-family dwelling). The local soil information in Richmond was gathered from Hunter et al. (1998) to obtain the average shear-wave velocity in the uppermost 30 m V_{s30} at building sites; the constructed contour map of V_{s30} for the Fraser River Delta region is shown in Fig. 2. The result indicates that the site class at the building sites is close to the site class D/E boundary, ranging from $V_{s30} = 160$ to 230 (m/s); hence, V_{s30} is modeled as a lognormal variate with the mean equal to 200 m/s and the coefficient of variation (CoV) equal to 0.075.

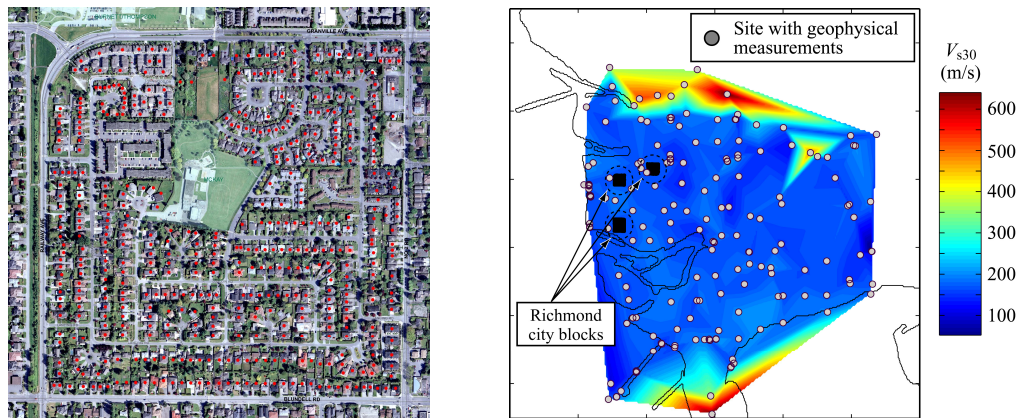


Figure 2. Aerial photo of one of the three city blocks in Richmond (a red dot represents a building), and contour map of the average shear-wave velocity in the uppermost 30 m V_{s30} in the Fraser River Delta region.

To incorporate the building information into the seismic risk model, association of the structural and use types defined by the City of Richmond with the HAZUS structural and occupancy types is carried out (Onur 2001; FEMA and NIBS 2003). The unit replacement costs are estimated based on FEMA and NIBS (2003), which do not necessarily reflect market/taxation values of the considered buildings; they are considered to be lognormally distributed with the CoV equal to 0.3. The total replacement cost of the 1574 buildings amounts to 734.8 million Canadian dollars (CAD). The natural vibration period T_n is determined according to Onur (2001) and White and Ventura (2007); for the majority of wood-frame houses, T_n is set to 0.4 seconds. The design base shear coefficient C_s is set to 0.160 (Onur 2001; FEMA and NIBS 2003), which corresponds to V_d in Panel 4 of Fig. 1; in addition, an over-strengthening

factor of 2.0, which corresponds to R_N in Panel 4 of Fig.1, is taken into account to define the yield displacement capacity D_R . The structural capacity parameters, yield displacement D_R and ultimate displacement μ_R , are considered to be lognormally distributed. The mean of D_R depends on C_s and R_N , and the mean of μ_R is set to 8.0, whereas the CoV of D_R and μ_R is set to 0.15 and 0.3, respectively; the parameters were selected according to available information in the literature (Onur 2001; FEMA and NIBS 2003; White and Ventura 2007).

Inelastic Seismic Demand Model for Various Hysteretic Characteristics

The inelastic seismic demand is estimated based on statistical prediction models that were developed from numerous nonlinear dynamic analyses using California records (Goda et al. 2009) and using Japanese records (Goda and Atkinson 2009b). To take complicated hysteretic characteristics of wood-frame structures into account, an inelastic SDOF system based on the Bouc-Wen model (Wen 1976) was adopted, which incorporates degradation and pinching effects. To determine adequate hysteretic parameters of the Bouc-Wen model, calibration is carried out by using the result obtained from the CASHEW model (Folz and Filiatrault 2001; White and Ventura 2007). For this, system identification based on the differential evolution algorithm (Ma et al. 2006) was implemented; the comparison of the force-deformation curve based on the CASHEW model with that based on the calibrated Bouc-Wen model is illustrated in Fig. 3.

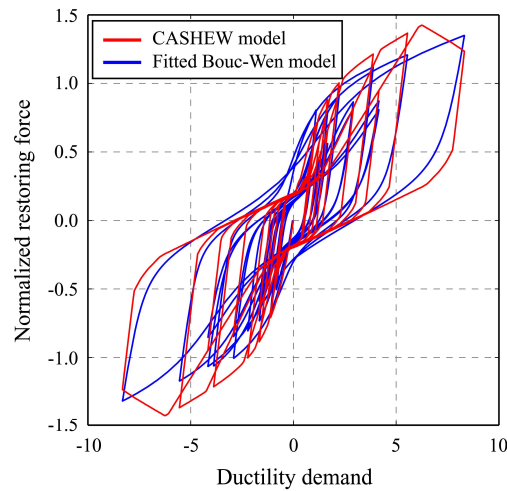


Figure 3. Comparison of the force-deformation curve based on the CASHEW model and the force-deformation curve based on the calibrated Bouc-Wen model.

Seismic Loss Estimation of 1574 Wood-frame Buildings

Calculation Cases

Seismic loss estimation is carried out by considering eight cases in total; brief summaries of the cases are shown in Table 2. Case 1 considers multiple GMPEs, spatial correlation models by Goda and Hong (2008a) and Goda and Atkinson (2009a), peak ductility demand prediction equations based on the calibrated Bouc-Wen model (Goda et al. 2009; Goda and Atkinson 2009b), and mean ultimate ductility capacity of 8.0. Other cases are associated with slightly

different model components with respect to Case 1 to investigate the impact of varied components on the estimated aggregate seismic loss. In Table 2, to briefly show the sensitivity results, the statistics of the annual aggregate seismic loss of the 1574 wood-frame buildings are provided.

Table 2. Seismic loss estimation cases and statistics of the annual aggregate seismic loss.

Case	GMPEs	Correlation model	Hysteretic model	Mean of μ_R	Annual occurrence rate	Mean of annual loss (1000 CAD)	Standard deviation of annual loss (1000 CAD)
Case 1	Multiple	Partial	Calibrated**	8.0	0.0558	985.2	13075.4
Case 2	Single	Partial	Calibrated**	8.0	0.0702	1406.4	16324.9
Case 3	Multiple	Partial*	Calibrated**	8.0	0.0621	981.9	12181.7
Case 4	Multiple	No	Calibrated**	8.0	0.1132	1004.7	9760.6
Case 5	Multiple	Full	Calibrated**	8.0	0.0260	978.8	15380.3
Case 6	Multiple	Partial	Bilinear	8.0	0.0477	789.9	11583.5
Case 7	Multiple	Partial	Calibrated**	6.0	0.0558	1219.6	15687.2
Case 8	Multiple	Partial	Calibrated**	10.0	0.0558	835.0	11314.9

* The correlation model by Goda and Hong (2008a) only is used.

** The calibrated Bouc-Wen model, shown in Fig. 3, is used.

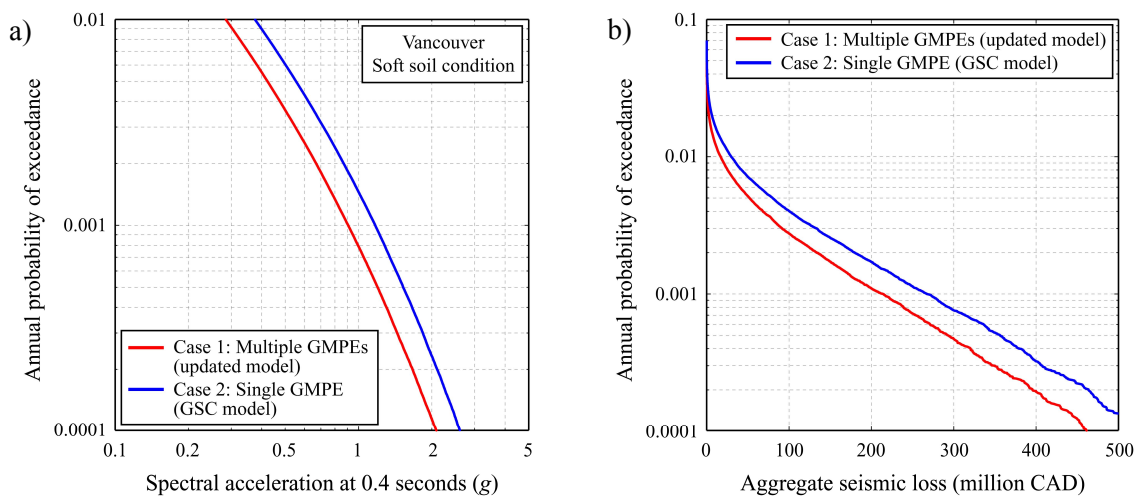


Figure 4. Comparison of the seismic hazard and risk assessments for Case 1 and Case 2: a) seismic hazard curve and b) seismic risk curve.

Impact of Multiple Ground Motion Prediction Equations (Case 1 versus Case 2).

The use of recently-developed GMPEs, together with proper distance measure conversion, results in significantly lower seismic hazard estimates than those based on the GSC model (Goda et al. 2010). To show this clearly, seismic hazard curves for the spectral acceleration at 0.4 seconds in Vancouver (soft soil condition with $V_{s30} = 200$ (m/s)) are compared in Fig. 4a. Furthermore, seismic risk curves (i.e., annual exceedance probability curve of the aggregate seismic loss of the 1574 wood-frame buildings) for Case 1 and Case 2 are compared in Fig. 4b. The results shown in Fig. 4 indicate that overestimation of seismic hazard (i.e., elastic seismic demand) leads to overestimation of the aggregate seismic loss by about (up to) 20-30% for the same probability level; thus, it is important to adopt suitable sets of multiple GMPEs for accurate seismic loss estimation.

Impact of Spatial Correlation Model (Case 1 versus Cases 3, 4, and 5).

The importance of using an adequate spatial correlation model of seismic excitations in seismic loss estimation of spatially distributed buildings has been demonstrated by Goda and Hong (2008b) for a hypothetical building inventory. To show the impact of the spatial correlation model for the 1574 wood-frame buildings, seismic risk curves for Cases 1, 3, 4, and 5 are compared in Fig. 5a. The results shown in Fig. 5a clearly indicate that the choice of the spatial correlation model has a significant influence on the seismic risk curve, especially at low exceedance probability levels. The use of the Goda-Atkinson model, rather than the Goda-Hong model, for inslab and interface subduction earthquakes results in more correlated aggregate seismic loss, as the former predicts a higher spatial correlation than the latter. One thing to be noted in interpreting these results is that the manipulation of the spatial correlation of seismic excitations alters the probability distribution of the aggregate seismic loss but preserves its expected value (see Table 2). This impact is different from those due to the use of multiple GMPEs (Fig. 4b) and different hysteretic models and seismic capacities (Fig. 5b).

Impact of Hysteretic Model and Seismic Capacity (Case 1 versus Cases 6, 7, and 8).

The use of an adequate hysteretic model and a reasonable ultimate seismic capacity has a direct impact on the seismic demand estimation and vulnerability assessment. In general, a degrading structural system with pinching behavior undergoes a higher inelastic seismic demand than a standard bilinear structural system. Furthermore, in the adopted seismic risk model, the seismic capacity μ_R defines the ultimate limit state for building replacement and determines the degree of damage severity δ for a given earthquake loading. To investigate the impact of using a simpler bilinear hysteretic model and of assuming a different mean seismic capacity, seismic loss estimation is carried out by considering Cases 6, 7, and 8. The obtained seismic risk curves are compared with that for Case 1 in Fig. 5b. We conclude that negligence of degradation and pinching behavior of a wood-frame building results in underestimation of the aggregate seismic loss by about (up to) 5-15% for a given probability level. The impact of the mean ductility capacity can be significant; the consideration of the mean ductility capacity of 6.0 or 10.0, instead of 8.0, could lead to overestimation or underestimation of the aggregate seismic loss by about (up to) 15-20%.

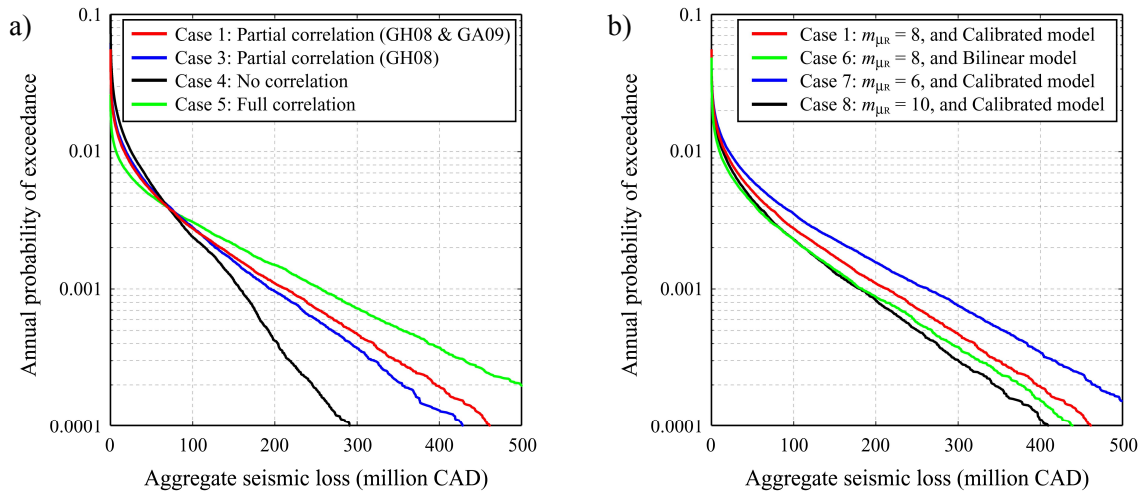


Figure 5. Comparison of the seismic risk curves: a) Case 1 versus Cases 3, 4, and 5 (impact of spatial correlation models) and b) Case 1 versus Cases 6, 7, and 8 (impact of hysteretic model and seismic capacity).

Summary and Conclusions

The seismic risk model for multiple buildings, which was originally developed by Goda and Hong (2008b), is updated to incorporate new seismic information, ground motion models, spatial correlation models of seismic effects, and peak inelastic ductility models of degrading structural systems with pinching behavior. The updated seismic risk model is then applied to 1574 existing wood-frame buildings, located in Richmond, British Columbia, to assess the probabilistic characteristics of the aggregate seismic loss and to investigate the sensitivity to varied model components. The analysis results indicate that the consideration of suitable sets of multiple GMPEs as well as realistic hysteretic characteristics affects the seismic risk curve to some extent. Most importantly, the use of an adequate spatial correlation model of peak ground motions and the determination of the expected seismic capacity have significant impacts on the seismic risk curve. Therefore, these two model components should be examined more thoroughly and elaborated/updated in future studies.

Acknowledgments

The financial support as well as the postdoctoral fellowship award provided for the first author by the Natural Sciences and Engineering Research Council of Canada is gratefully acknowledged. We thank Lorin Gaertner and the City of Richmond for providing us with the building inventory information.

References

- Adams, J., and S. Halchuk, 2003. Fourth generation seismic hazard maps of Canada: values for over 650 Canadian localities intended for the 2005 National Building Code of Canada, Open-File 4459, Geological Survey of Canada, Ottawa, Canada.
- Atkinson, G. M., and D. M. Boore, 2003. Empirical ground-motion relations for subduction-zone earthquakes and their application to Cascadia and other regions, *Bull. Seism. Soc. Am.* 93 (4),

1703-1729.

- Atkinson, G. M., 2005. Ground motions for earthquakes in southwestern British Columbia and northwestern Washington: crustal, in-slab, and offshore events, *Bull. Seism. Soc. Am.* 95 (3), 1027-1044.
- Atkinson, G. M., and M. Macias, 2009. Predicted ground motions for great interface earthquakes in the Cascadia subduction zone, *Bull. Seism. Soc. Am.* 99 (3), 1552-1578.
- Boore, D. M., and G. M. Atkinson, 2008. Ground-motion prediction equations for the average horizontal component of PGA, PGV, and 5%-damped PSA at spectral periods between 0.01 s and 10.0 s, *Earthquake Spectra* 24 (1), 99-138.
- Federal Emergency Management Agency (FEMA), and National Institute of Building Sciences (NIBS), 2003. HAZUS-Earthquake - Technical Manual, Federal Emergency Management Agency and National Institute of Building Sciences, Washington D.C.
- Folz, B., and A. Filiatrault, 2001. Cyclic analysis of wood shear walls, *J. Structural Eng.* 127 (4), 433-441.
- Goda, K., and H. P. Hong, 2008a. Spatial correlation of peak ground motions and response spectra, *Bull. Seism. Soc. Am.* 98 (1), 354-365.
- Goda, K., and H. P. Hong, 2008b. Estimation of seismic loss for spatially distributed buildings, *Earthquake Spectra* 24 (4), 889-910.
- Goda, K., and G. M. Atkinson, 2009a. Probabilistic characterization of spatially-correlated response spectra for earthquakes in Japan, *Bull. Seism. Soc. Am.* 99 (5), 3003-3020.
- Goda, K., and G. M. Atkinson, 2009b. Seismic demand estimation of inelastic SDOF systems for earthquakes in Japan, *Bull. Seism. Soc. Am.* 99 (6), 3284-3299.
- Goda, K., H. P. Hong, and C. S. Lee, 2009. Probabilistic characteristics of seismic ductility demand of SDOF systems with Bouc-Wen hysteretic behavior, *J. Earthquake Eng.* 13 (5), 600-622.
- Goda, K., H. P. Hong, and G. M. Atkinson, 2010. Impact of using updated seismic information on seismic hazard in western Canada, *Canadian J. Civil Eng.* 37 (in press).
- Gregor, N. J., W. J. Silva, I. G. Wong, and R. R. Youngs, 2002. Ground-motion attenuation relationships for Cascadia subduction zone megathrust earthquakes based on a stochastic finite-fault model, *Bull. Seism. Soc. Am.* 92 (5), 1923-1932.
- Hong H. P., and K. Goda, 2007. Orientation-dependent ground-motion measure for seismic-hazard assessment, *Bull. Seism. Soc. Am.* 97 (5), 1525-1538.
- Hunter, J. A., R. A. Burns, R. L. Good, and C. F. Pelletier, 1998. A compilation of shear wave velocities and borehole geophysical logs in unconsolidated sediments of the Fraser River Delta, Open-File 3622, Geological Survey of Canada, Ottawa, Canada.
- Ma, F., C. H. Ng, and N. Ajavakom, 2006. On system identification and response prediction of degrading structures, *Structural Control Health Monitoring* 13 (1), 347-364.
- Onur, T., 2001. Seismic risk assessment in south western British Columbia, Ph.D. Thesis, University of British Columbia, Vancouver, Canada.
- Scherbaum, F., J. Schmedes, and F. Cotton, 2004. On the conversion of source-to-site distance measures for extended earthquake source models, *Bull. Seism. Soc. Am.* 94 (3), 1053-1069.
- Wen, Y. K., 1976. Method for random vibration of hysteretic systems, *J. Eng. Mech.* 102 (2), 249-263.
- White, T. W., and C. E. Ventura, 2007. Seismic behaviour of residential wood-frame construction in British Columbia: Part I – modeling and validation, *9th Canadian Conference on Earthquake Eng.*, Ottawa, Canada, 935-944.
- Zhao, J. X., J. Zhang, A. Asano, Y. Ohno, T. Oouchi, T. Takahashi, H. Ogawa, K. Irikura, H. K. Thio, P. G. Somerville, Y. Fukushima, and Y. Fukushima, 2006. Attenuation relations of strong ground motion in Japan using site classification based on predominant period, *Bull. Seism. Soc. Am.* 96 (3), 898-913.